ISSN (Print) 1226-1750
ISSN (Online) 2233-6656
Journal of Magnetics 22(3), 395-405 (2017) https://doi.org/10.4283/JMAG.2017.22.3.395

Analytical Method for the Magnetic Field Line Distribution of a Fan-shaped Permanent Magnet and the Calculation of Leakage Permeance

H. M. Liang[1], K. Zhang[1], J. X. You[1]*, F. B. Luo[2], and Z. W. Cai[2]

[1]*Harbin Institute of Technology, Harbin 150001, China*
[2]*GuiLin Aerospace Technologies Co., Ltd. GuiLin 541002, China*

(Received 26 December 2016, Received in final form 19 May 2017, Accepted 16 June 2017)

Leakage permeance of a permanent magnet (PM) is an important factor for improving the accuracy of electromagnetic device calculations based on a magnetic equivalent circuit (MEC). For PM leakage permeance calculations, the traditional simulation method of finite element analysis (FEA) and the lumped parameter analytical method (LPAM) have been considered; it was found that FEA has the disadvantage of a long calculation time and LPAM has low accuracy. The magnetic field lines distribution analytical method (MFLD) is proposed in this paper in order to raise computational efficiency and keep accuracy within a certain range. The electromagnetic features of open circuit fan-shaped PMs are presented by MFLD and finite element analysis (FEA) is adopted to match the MFLD results. In order to verify the validity of the proposed method in a magnetic system, the working points of PMs in an electromagnetic actuator are calculated, and the numerical results compared with the experimental results.

Keywords : electromagnetic actuator, fan-shaped permanent magnet, finite element analysis, leakage permeance

1. Introduction

The characteristics of an electromagnetic system with permanent magnets (PMs) can be obtained by magnetic equivalent circuit equations (MECs). However, the error of its calculation result is large, because the PM's analytical model is simplified as magnetic potential and reluctance in the magnetic system. In practice, the PM's working points are different and leakage flux exists in the surface. The simplifications often mean that the electric appliance designer has to face low accuracy from the conventional MEC model and compensation or correction relies only on experiential theory and formulae generalized from practice. Therefore, in order to improve the accuracy of MEC calculations, the equations require leakage permeance of the PM. The distribution of magnetic field lines is the important characteristic of PMs and electromagnetic systems, which is closely related to leakage permeance. In general, the cylindrical electromagnetic valve and electrical machine have fan-shaped PMs. The characteristics of the magnetic field lines distribution can be clarified using a case study of an open circuit fan-shaped PM. Using this as a basis, the characteristics of an electromagnetic system can be obtained by developing a high accuracy model. Often, the sketch of the electric field equipotential and magnetic field lines are parallel and interchanged regularly by two parallel infinite wires with opposite charges [1].

Some researchers have done a lot of work on fast calculations for electromagnetic systems with PMs using mathematical models [2-5]. In some cases, the calculations focus on the characterization of bar PM magnetic field lines distribution in the electromagnetic system, which simplifies the processes of the operations based on the calculation of leakage permeance, thus making it easier to understand [6-8]. The research on electromagnetic systems with fan-shaped PM is mainly focused on motor field based on FEA to acquisition of motor systemic characterization [9-12]. However, there is not much academic research on magnetic field lines distribution and leakage permeance of open circuit fan-shaped PMs. Birch and Butler studied the effects of permeance of closed-slot bridges on induction-motor-current computation [13]. Bao analyzed the slot leakage reactance of a submersible motor [14]. Flux leakage was calculated by Li and Chau [15], where the possible flux paths of a PM linear vernier

*Corresponding author: Tel: +86-0451-86413193
Fax: +86-0451-86413964, e-mail: 3240569595@qq.com

machine were analyzed and identified with an ideal flux source, making it suitable only for bar PMs. FEA has become the first choice of method for electromagnetic calculations on account of its great applicability and accuracy [16-23]; however, FEA cannot obtain the exact results with a low computational cost. The lumped parameter analytical method (LPAM) of an electromagnetic system depends solely on simple empirical formulae and these calculations are very imprecise. Moreover, the conventional method is expected to work only in ideal circumstances, requiring an infinite line or a PM with enough width so that it will not affect the distribution; when space direction is perpendicular to the plane of the sketch for the magnetic field lines, the relationship between them becomes complicated and there is no systematic or comprehensive research in this field so far.

In this paper, the magnetic field lines distribution (MFLD) analytical method is presented for the calculation of leakage permeance of fan-shaped PMs to save computation time whilst guaranteeing accuracy. To provide accuracy of the calculation of leakage permeance, the PM is divided into several segments for calculation. The magnetic field lines of open circuit fan-shaped PMs are mapped based on the superposition principle of magnetic fields. Then, the positions of segmented PMs can be obtained based on the magnetic field lines distribution. The volumes and average lengths of flux tubes were required to obtain the leakage permeance of segmented PMs with the permeance formula. In the case of open circuit PMs, the accuracy and computation cost of the proposed method is verified by comparing the results obtained by FEA and LPAM. An electromagnetic actuator is employed to verify the validity of the proposed method in electromagnetic systems, and the measured results from the FEA and LPAM are compared with the MFLD result.

2. The Magnetic Field Lines

2.1. Characteristics of permanent magnets

Sintered rare-earth Nd-Fe-B was selected as the fan-shaped PM material; it can be simulated and analyzed, showing the following properties: $Br = 1.15$T, $Hc = 896$ kA/m, and $R_1 = 9$ mm, $R_2 = 18.5$ mm; where R_1 and R_2 are the inner and outer radius, respectively. The fan-shaped PM opening angle is 20° and it is magnetized in the radial direction, with the *S* pole for the inner radius. PM height is set as a variable. Figure 1(a). shows a three-dimensional illustration of the PM, and the fan-shaped surface in the front side, which is perpendicular to the flank side and the inner side is the *S*-pole.

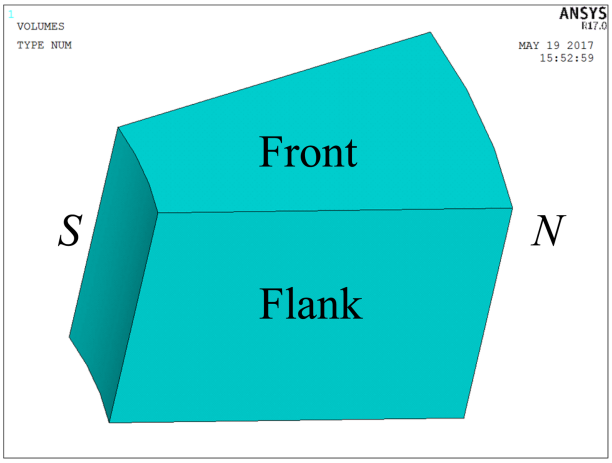

(a)

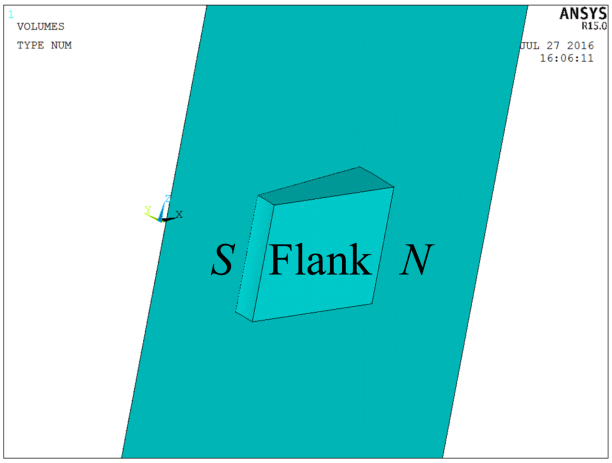

(b)

Fig. 1. (Color online) (a) Open circuit fan-shaped PM in 3D FEA software; (b) longitudinal interception by the air layer.

2.2. Longitudinal PM magnetic field lines

In order to acquire reliable curves and leakage magnetic data, an air layer has to be built which is extremely thin but with enough length and height. Figure 1(b) shows a rectangle air layer cut in a PM of 8 mm height in longitudinal and across the geometric center.

The conventional 2D magnetic field lines in FEA software are not applicable to the fan surface of PMs, due to divergence of the magnetic field. As a consequence of this, the vector line is considered. The 3D vector lines are shown in Fig. 2, from which the data and curves can be obtained. The magnetic field line is a non-overlapping arc line, where the vertical points of peaks on the PM surface are in the central position on the magnetic field line. Table 1 shows the different PM heights and distances between the central position of the innermost line and inner radius.

The center of the outermost magnetic field line should,

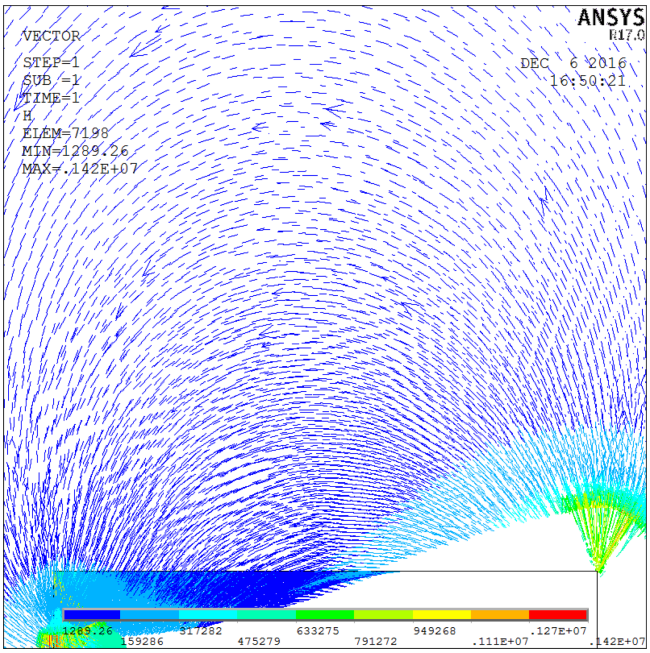

Fig. 2. (Color online) The vector line on the longitudinal air layer.

Table 1. Distance between the central position of the innermost line and the inner radius with different PM heights.

PM height (mm)	2D magnetic field lines (mm)	3DVector line (mm)
16	5.81	6.78
9.5	5.67	6.78
8	5.58	6.83
6	5.55	6.9
4	5.52	7.03
2	5.35	7.46
1	4.11	7.99

theoretically, be located at the perpendicular bisector of the PM in free space at infinity. Actually, the effect of PMs on a limited scale would be negligible. For this reason, the linear distance h_1 between the point and PM surface is large enough that the magnetic field is weak enough to be ignored. Figure 3 shows the distribution of lines on the front side by the analytical method; where, $h = R_2 - R_1$; h is the geometrical length of the PM; d takes into account Table 1, which is the central position of the innermost line subtracted by $h/2$; point O is the origin of coordinates; P_0 is the peak of the outer magnetic field line; P_1 is the peak of the outermost magnetic field line. Then, assume the peak of other magnetic field lines are on line P_0P_1. After the position of the magnetic field lines migrated, a full magnetic field line is a combinational curve of two arc lines. Line P_0P_1 is the boundary of the

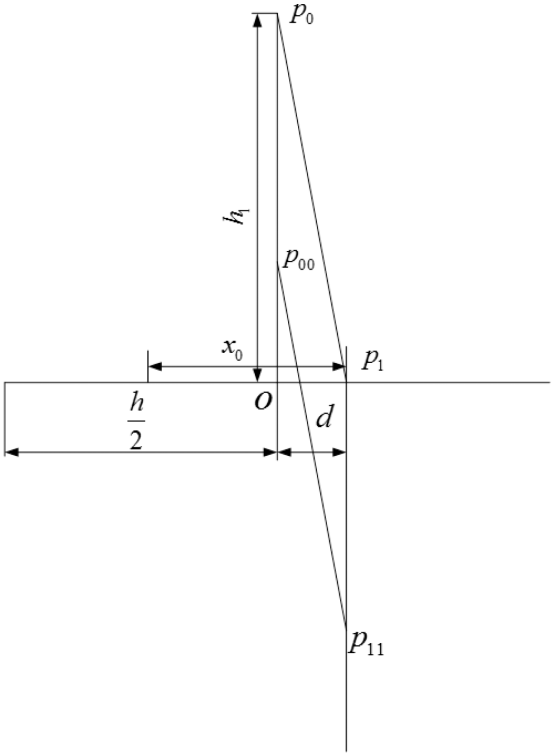

Fig. 3. Distribution of lines on the Front side using the analytical method.

two arcs, P_{00} is the center of the outermost magnetic field line and P_{11} is the center of the innermost magnetic field line; assuming the center of other magnetic field lines is on line $P_{00}P_{11}$, these two lines are parallel to each other.

According the superposition principle of magnetic fields, if the PM is parallel to two current-carrying wires, the arc of the magnetic field line is as follows [24]

$$x^2 + (y - y_0)^2 = y_0^2 + d_0^2 \tag{1}$$

Two constants y_0 and d_0 would be required to produce the arc. y_0 is the distance from the center of the arc to the x-axis. d_0 is the distance from the center of the wire to the y-axis.

According to trigonometric functions, the P_{00} coordinates on the plane are $(\frac{h_1}{2} - \frac{h^2}{8h_1}, 0)$, and $(-\frac{h_1}{2} - \frac{h^2}{8h_1}, 0)$ for P_{11}. According to the linear form formula, $y = kx + b$, the coordinates of P_{00} and P_{11} lines can be obtained by

$$y = -\frac{h_1}{d}x + \frac{h_1}{2} - \frac{h^2}{8h_1} \tag{2}$$

For a typical bar PM, the y-axis is fixed in a perpendicular bisector [25]; however, the position of the y-axis for every magnetic field line presents a gradient change for fan-shaped PMs. To address this problem, x_0 is

introduced to represent the distance from wire to P_{11}. x_0 can be changed with y in monotone decreasing and described mathematically by

$$\begin{cases} y = kx_0 + b \\ \dfrac{h_1}{2} - \dfrac{h^2}{8h_1} = k\left(\dfrac{h}{2} + \mathrm{d}\right) + b \\ -\left(\dfrac{h_1}{2} + \dfrac{h^2}{8h_1}\right) = b \end{cases} \tag{3}$$

According to (3), a linear relationship between x_0 and y can be given by

$$y = \frac{h_1}{d + \dfrac{h}{2}} x_0 - \left(\frac{h_1}{2} + \frac{h^2}{8h_1}\right) \tag{4}$$

Substituting (4) into (2), x_0 can be simplified to

$$x_0 = d + \frac{h}{2} - \left(1 + \frac{h}{2d}\right) x \tag{5}$$

d_0 can be expressed as

$$d_0 = x_0 - (d - x) = x_0 - x + d \tag{6}$$

Combining (2), (4), and (6), d_0 can be simplified to

$$d_0 = \frac{h}{2} - \frac{h}{2d} x \tag{7}$$

There is only one variable x in (7).

Combining (1), (2), and (7), the magnetic field line of the front side of the PM can be expressed as

$$\begin{aligned} &(x - x_m)^2 + \left(y + \frac{h_1}{d} x_m - \frac{h_1}{2} + \frac{h^2}{8h_1}\right)^2 \\ &= \left(\frac{h_1}{d} x_m - \frac{h_1}{2} + \frac{h^2}{8h_1}\right)^2 + \left(\frac{h}{2} - \frac{h}{2d} x_m\right)^2 \end{aligned} \tag{8}$$

Where x_m is the point on line $P_{00}P_{11}$, which can be calculated as follows

$$x_m(i) = \frac{d}{n}(i - 1) \tag{9}$$

Where n is the number of segmented, $i = 1, 2, 3, ..., n$.

Line P_0P_1 can be expressed as

$$y = -\frac{h_1}{d} x + h_1 \tag{10}$$

Formulae (8) and (10) can be used to obtain the point of intersection (x_{01}, y_{01}) on line P_0P_1, and $y_{01} > 0$. Substituting (9) into (10), allows y_m to be obtained.

When $y = 0$ in (8), the point of intersection (x_{02}, 0) on the surface of the front side can be obtained. x_{02} must be close to the inner radius. (x_{22}, 0) is set as the point of intersection close to the outer radius.

$$x_{22} = \frac{h}{2} - \frac{x_{02} + \dfrac{h}{2}}{\dfrac{h}{2} + d}(h - d) \tag{11}$$

x_{22} can be obtained by proportion transformation.

(x_{01}, y_{01}) and (x_{22}, 0) are known, and the perpendicular bisector of the line between the two points can be obtained by

$$y = \frac{x_{22} - x_1}{y_1} x + \frac{y_1}{2} + \frac{x_1^2 - x_{22}^2}{2y_1} \tag{12}$$

The center of arc (x_n, y_n) between the points can be obtained from (2) and (12), the arc can be obtained by

$$(x - x_n)^2 + (y - y_n)^2 = (x_{22} - x_n)^2 + y_n^2 \tag{13}$$

According to (8) and (13), the whole arc can be mapped.

2.3. Horizontal PM magnetic field lines

A rectangle air layer cut across the 8 mm height PM. The 2D magnetic field lines on the layer are shown in Fig. 4. The distribution of 3D vector lines has an effect similar to 2D magnetic field lines. Figure 5 shows the distribution of lines on the Flank side using the analytical method. Where the magnetic field lines come out from

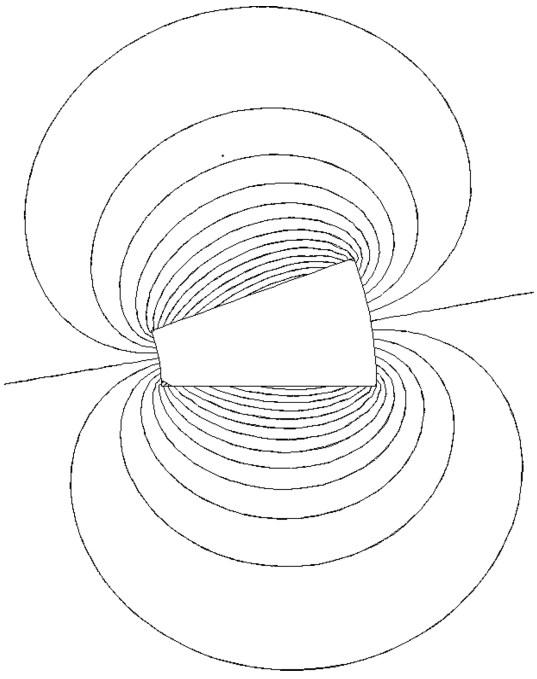

Fig. 4. Distribution of lines on the Front side using the 2D FEA method.

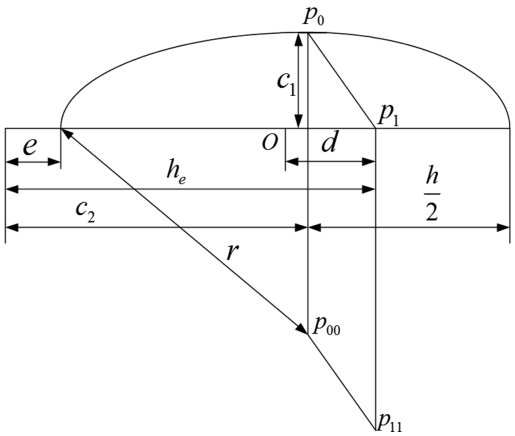

Fig. 5. Distribution of lines on the Flank side using the analytical method.

the inner radius, and do not come back to the PM surface but the outer radius end. There are some differences from Fig. 3:

1) The distance from the initial position of the magnetic field line to the inner radius is e.

2) The distance from the center position of the outer magnetic field line to the inner radius is c_2.

3) The distance from P_1 to the inner radius is he.

4) The height of the outer magnetic field line is c_1.

5) $d = h_e - e - h/2$.

Line $P_{00}P_{11}$ can be written a

$$y = \frac{c_1}{c_1 - e - \frac{h}{2} - d} x - \frac{c_1\left(c_2 - e - \frac{h}{2}\right)}{c_2 - e - \frac{h}{2} - d} - r - c_1 \tag{14}$$

The relationship between x_0 and y can be given by

$$y = \frac{c_1}{\frac{h}{2} + d} x_0 - r \tag{15}$$

Substituting (14) into (15), x_0 can be written as

$$x_0 = \frac{c_1}{c_2 - e - \frac{h}{2} - d} x + \frac{h}{2} + d - \frac{\left(c_2 - e - \frac{h}{2}\right)\left(\frac{h}{2} + d\right)}{c_2 - e - \frac{h}{2} - d} \tag{16}$$

Substituting (16) into (6), d_0 can be simplified to

$$d_0 = \frac{c_1}{c_2 - e - \frac{h}{2} - d} x + \frac{h}{2} - \frac{\left(c_2 - e - \frac{h}{2}\right)\left(\frac{h}{2} + d\right)}{c_2 - e - \frac{h}{2} - d} \tag{17}$$

x_m can be expressed as

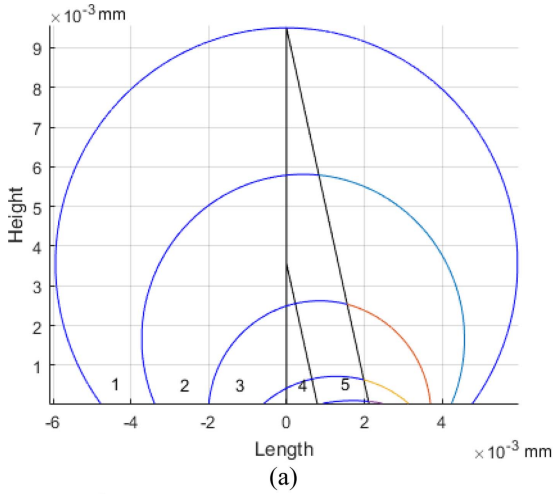

(a)

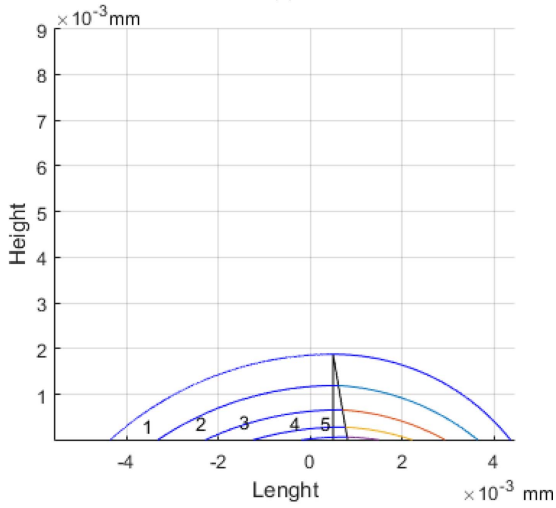

(b)

Fig. 6. (Color online) (a) The magnetic field lines of the Front side; (b) the magnetic field lines of the Flank side.

$$x_m(i) = \frac{d - c_2 + e + \frac{h}{2}}{n} i + c_2 - e - \frac{h}{2} \tag{18}$$

Line P_0P_1 can be expressed as

$$y = \frac{c_1}{c_1 - e - \frac{h}{2} - d} x - \frac{d \cdot c_1}{c_2 - e - \frac{h}{2} - d} \tag{19}$$

The analytical method is the same as the longitudinal of PM magnetic field lines. Figure 6(a) and Fig. 6(b) show that the magnetic field lines of the Front and Flank side are mapped by the analytical method in 5 segments.

3. Calculation of Leakage Permeance

3.1. Calculation method based on magnetic field lines

The calculation of segmented leakage permeance (related

to the volume and length of flux tube) is based on magnetic field lines. The PM was divided into 5 segments; the segmented position with no PM height change, on account of d, has limited range and d_0 only relates to x, which determines its stationarity.

The segmented volumes of the Front side can be obtained

$$V = \int \frac{\pi(r_1 + r_2)\alpha}{360} S_m ds \tag{20}$$

Where a is the angle of the fan-shaped PM, and S_m is the area of each flux tube.

The segmented volumes of the Flank side can be obtained by

$$V = \oint h_{pm} S_m ds \tag{21}$$

Where h_{pm} is the height of the PM.

According to (20) or (21), leakage permeance can be calculated by the permeance formula

$$G = \int \frac{\mu_0 V}{A l_p^2} dv \tag{22}$$

Where l_p is the average length of the magnetic flux tube, which can be obtained from (8) and (13). A is the adjustment parameter, which is a variable that regulates the error change over PM height, angle, inner, and outer radius. For a conventional bar PM, when we change PMs by height, the width is an effective way to increase magnetic potential. Unfortunately, the effect of changing the PM angle is not obvious for fan-shaped PMs. In this paper, A is the only variable on PM to be height-related as change in PM height is more pronounced. It is obtained from [26].

$$A = a_1 x^2 + a_2 x + a_3 \tag{23}$$

A can be obtained from the formula (23), where x is the PM height, and $a_1 = -0.07921$, $a_2 = 0.2211$, and $a_3 = 0.8577$, when A is calculated for the Front side; but $a_1 = -0.09392$, $a_2 = 0.01569$, and $a_3 = 0.9449$, when A is calculated for the Flank side.

The leakage permeance of oblique incidence can be given by [27].

$$G_f = 0.6366 \mu_0 (r_2 - r_1) \tag{24}$$

Where r_1 and r_2 are the inner and outer radii, respectively.

3.2. The lumped parameter analytical method

The permeance of the Front side can be considered as the average values of the two bar PMs. It can be obtained by

$$G_{fr} = \mu_0 \frac{V}{l_p^2} = 0.26 \mu_0 \left(\frac{l_1 + l_2}{2} \right) \tag{25}$$

Where l_1 is the arc length of the inner radius, and l_2 is the arc length of the outer radius.

The permeance of the Flank side can be obtained by [27].

$$G_{fl} = 0.26 \mu_0 h_{pm} \tag{26}$$

Where h_{pm} is the height of the PM. The formula of leakage permeance of the Flank side can be obtained by (25) for the semi-cylinder flux tube of leakage permeance. The leakage permeance of oblique incidence can be obtained by (24).

3.3. Analysis of leakage permeance data

The results from the MFLD and FEA predictions of segmented leakage permeance are shown in Fig. 7. Figure 7(a) shows the Flank side data comparison of leakage permeance, and the MFLD prediction is compared with

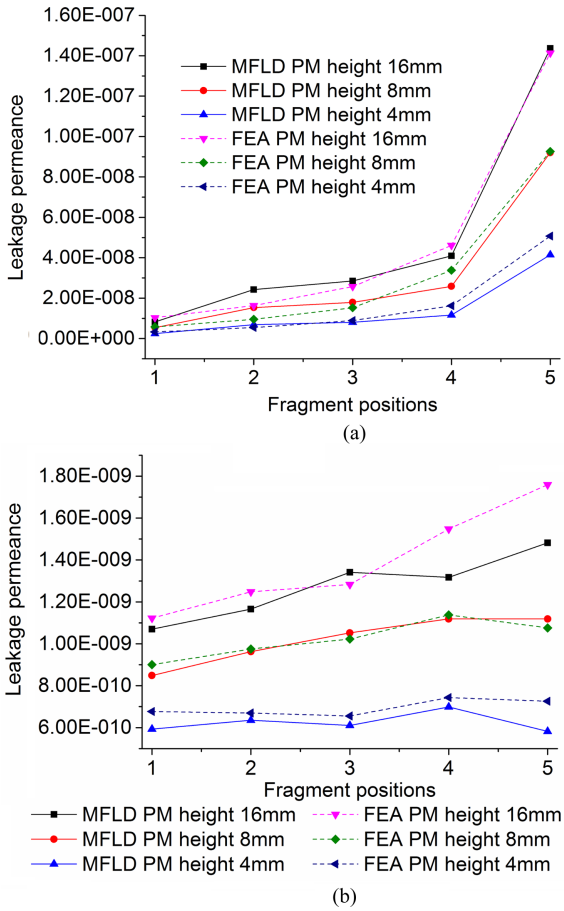

Fig. 7. (Color online) (a) Flank side leakage permaeance of MFLD and FEA results; (b) Front side leakage permeance of MFLD and FEA results.

Table 2. Total leakage permeance of FEA MFLD and LPAM.

PM high (mm)	Leakage permeance (10^{-7} H)			FEA-MFLD Error
	FEA	MFLD	LPAM	
16	2.47	2.59	0.141	4.9%
9.5	1.66	1.8	0.12	8.4%
8	1.62	1.69	0.115	4.3%
6	1.17	1.19	0.108	1.7%
4	0.881	0.81	0.102	8.1%
2	0.437	0.41	0.0951	6.2%

the FEA prediction. As is shown, the effect of permeance increases with position and the predicted permeance by the MFLD with different PM heights almost completely matches the FEA results. Exceptions are the curves of the 16 mm and 4 mm PM heights. MFLD and FEA are not well-matched for these heights, as seen in Fig. 7(b), because a PM height that is too long or too short will significantly reduce the measuring accuracy of magnetic field lines. Additionally, the ambiguous boundaries at 2/3 PM length refers to the PM height range which is supposed to obtain a good result; beyond this range, calculating accurate leakage permeance data is difficult. Not only that, the leakage permeance in Fig. 7(b) is much less than that in Fig. 7(a), which suggests that leakage permeance mainly centralizes on the Flank side. Therefore, in order to simplify the calculating processes, the Front side leakage permeance can be ignored, and the leakage permeance of a PM can be obtained by

$$G(i) = \frac{\mu_0 h_{pm}}{A} \frac{S(i) - S(i+1)}{\left(\frac{l_t(i) + l_t(i+1)}{2} \right)^2} \tag{27}$$

Where l_t is the total arc length, and $l_t = l_{left} + l_{right}$, where l_{left} and l_{right} represent the left and right arc lengths, respectively. S is the area enclosed by the arc and PM surface. It can be given according to a series of arc and triangle area formulas. Table 2 shows the total leakage permeance of the LPAM, FEA, and MFLD results. The FEA-MFLD error is under 10 %; however, the LPAM results have large errors, because the influence of the PM length or shape on the magnetic field line distribution was not considered (this is especially important when the PM shape is not a common bar). The Matlab running time for LPAM is 1 second, MFLD is 5 seconds, while the FEA software running time is 485 seconds (all using the same PC hardware).

4. The Electromagnetic Actuator

A system model is important for calculating and analyzing leakage permeance. In this paper, an electromagnetic actuator model is developed and the model is devoted to the electromagnetic valve actuator. As demonstrated in Fig. 8, the actuator is composed of two sets of PMs, coils, armatures, covers and shells. The up actuator is A, and the low actuator is B, where the sleeve is a nonmagnetic material which contacts A and B. The overall physical parameters of the designed electromagnetic actuator are summarized in Table 3. The 2D model of the actuator was established using FEA software. Figure 9(a) shows the basic structure of the actuator and the 2D magnetic field lines distribution of the longitudinal section, where the rectangular boxes are PMs, the cone

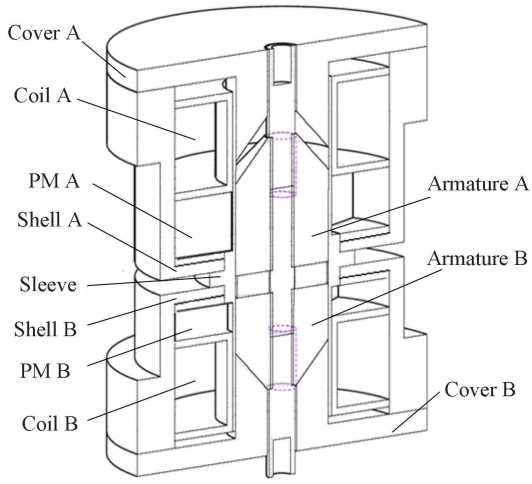

Fig. 8. (Color online) Structure diagram of the electromagnetic actuator.

Table 3. Actuator design features.

Components		Features
Shell	outer diameter	42 mm
Shell	inner diameter	37 mm
Shell A	height	26 mm
Shell B	height	21.5 mm
Coil	height	14 mm
Coil	resistance	8.55Ω
Coil	turns	550
Coil	voltage	28 v
PM A	height	8 mm
PM A	quantity	16
PM B	height	4 mm
PM B	quantity	13
PM	outer diameter	37 mm
PM	inner diameter	17 mm
PM	angle	20°
PM	Hc	896 KA/m
PM	Br	1.15T

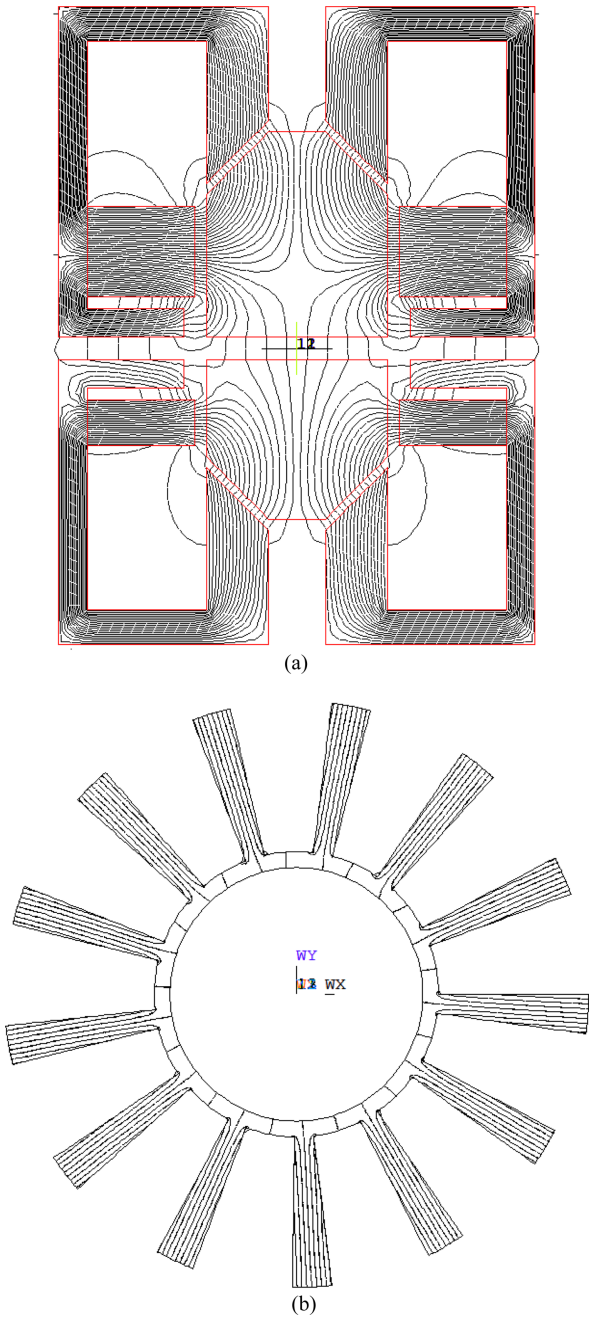

(a)

(b)

Fig. 9. (Color online) (a) 2D magnetic field lines distribution of the longitudinal section of the actuator; (b) 2D magnetic field lines distribution of the horizontal section of the actuator.

armature is the moving part with 2 mm strokes, the upward movement is positive movement, and the top position is set as the end of the stroke. Figure 9(b) shows the 2D magnetic field lines distribution of the horizontal section of the actuator. The Front and Flank side leakage permeance can be obtained using the magnetic field lines distribution.

Only Flank side leakage permeance has been considered in this paper. The longitudinal section of the actuator clearance for PMs in the air layer is shown in Fig. 10(a) and the equivalent segmented figure is shown in Fig. 10(b), where α is the angle between the arc and the PM; and l_1, l_2,…, l_n represent the segmented lengths of the PM. The arc line can be simplified to straight lines because of narrow spaces among PMs.

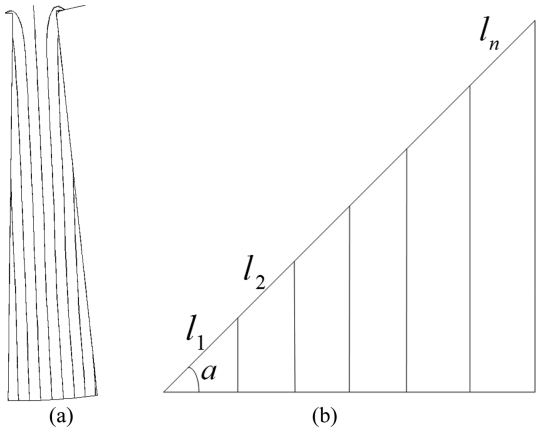

(a) (b)

Fig. 10. (a) The clearance for the PM in the air layer; (b) the equivalent figure for magnetic field lines of the PM.

According to the formula of permeance, both $V(i)$ and $l_p(i)$ are required, where $V(i)$ represents the volume of the flux tube, and $l_p(i)$ represents the average length of the magnetic field lines in the flux tube. The volume of the flux tube of the fan-shaped PM can be written as

$$V == \int S\pi \frac{a}{180}\left(\sum_{2}^{n} l(i) + \frac{l_1}{2}\right) ds \tag{28}$$

Where a is angle of the fan-shaped PM; $i = 1, 2, ..., n$. The arc line l_{arc} can then be obtained by

$$l_{arc}(i) = \frac{\pi((l_1 + l_2 + ... + l(i))^2 + (la_1 + la_2 + ... + la(i))^2)}{360(la_1 + la_2 + ... + la(i))} \times \arctan \frac{2(l_1 + l_2 + ... + l(i))(la_1 + la_2 + ... + la(i))}{((l_1 + l_2 + ... + l(i))^2 + (la_1 + la_2 + ... + la(i))^2)} \tag{29}$$

Then l_p can be obtained by the following formula

$$\begin{cases} l_p(i) = \dfrac{l_{arc}(i) + l_{arc}(i+1)}{2} \\ l_p(1) = \dfrac{l_{arc}(1)}{2} \end{cases} \tag{30}$$

Where i = 2, 3,…, n–1. Formulae (29) and (30) can be used to calculate the left and right side of the average length of the magnetic field lines calculation. Therefore, G can be obtained by combining (28), (29), and (30). The leakage permeance can be summarized into the following

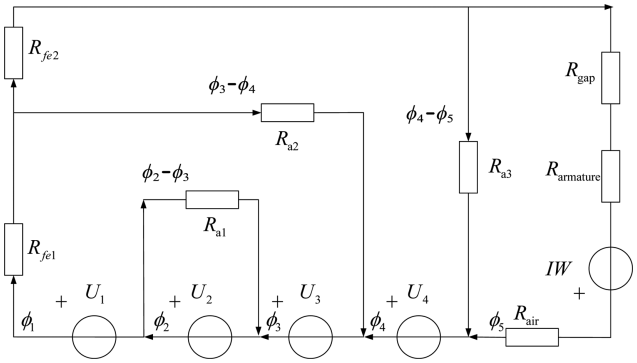

Fig. 11. Distributed parameter model of the actuator magnetic equivalent circuit.

formula

$$G(i)=\frac{2\mu_0 h\tan\alpha}{l^2(i)}\left[\left(\sum_1^n l(i)\right)^2-\left(\sum_1^{n-1} l(i)\right)^2\right] \tag{31}$$

Where h is the PM height. The force characteristics of electromagnetic actuator can be calculated in light of the distributed parameter model with PM leakage permeance. According to Fig. 9(a), the distributed parameter model of magnetic equivalent circuits is established and shown in Fig. 11, where U_1, U_2, U_3, and U_1 represent the magnetic pressure of four PM segments; ϕ_1, ϕ_2, ϕ_3, and ϕ_4 are the magnetic flux passing through PM segments; ϕ_5 is the magnetic flux passing through non-work air-gaps; R_{fe1}, R_{fe2}, R_{fe3}, and R_{fe4} are the magnetic resistance of the soft magnetic material segments; R_{gap} is the work air-gap's magnetic resistance; Ra_1, Ra_2, Ra_3, and Ra_4 represent the air leakage's magnetic resistance; $\phi_1-\phi_2$, $\phi_2-\phi_3$, $\phi_3-\phi_4$, and $\phi_4-\phi_5$ are the magnetic flux passing through the air leakage's magnetic resistance; and IW is the ampere-turns provided by the coil. To obtain an accurate flux density distribution on the PM, the Newton iteration process was employed to update the material's permeability. According to flux density, the flux can be obtained by an equivalent magnetic circuit.

The force of the actuator can be calculated by the Maxwell electromagnetic force formulae.

$$P=\frac{\phi_{up}^2-\phi_{down}^2}{2\mu_0 S_A}\cos\theta \tag{32}$$

Where ϕ_{up}, ϕ_{down} represent the flux passing through armature A and B, corresponding to ϕ_5 in Fig. 11; S_A is the polar area of the work air-gap; θ is the cone angle of the armature; and P represents force.

Figure 12 shows the latching and output force of the actuator under 0AT, 1800AT, and −1800AT. The results from Fig. 10(b) show a qualitatively good agreement,

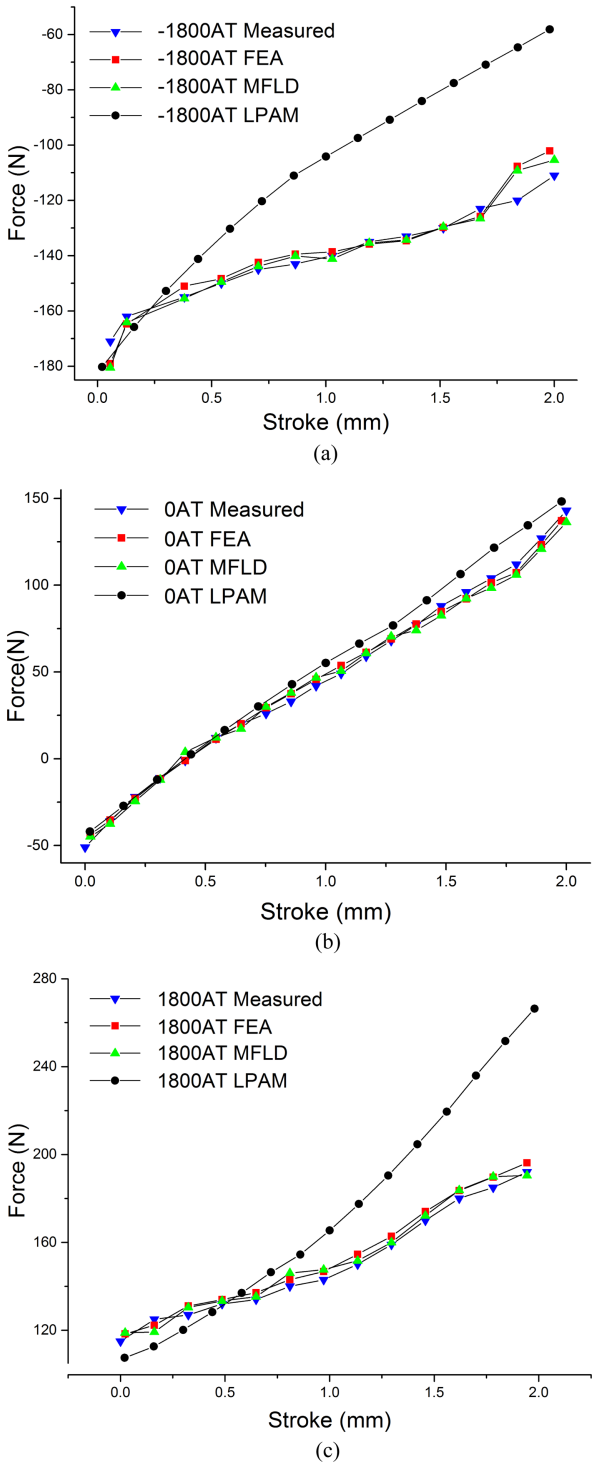

Fig. 12. (Color online) (a) The output force of the actuator under −1800 ampere-turns; (b) the latching force of theactuator under 0 ampere-turns; (c) the output force of the actuator under 1800 ampere-turns.

because the leakage permeance has limited effect on the latching force of the actuator under 0AT when the PM is in this magnetic system. From Fig. 11(a) and (c), it can be

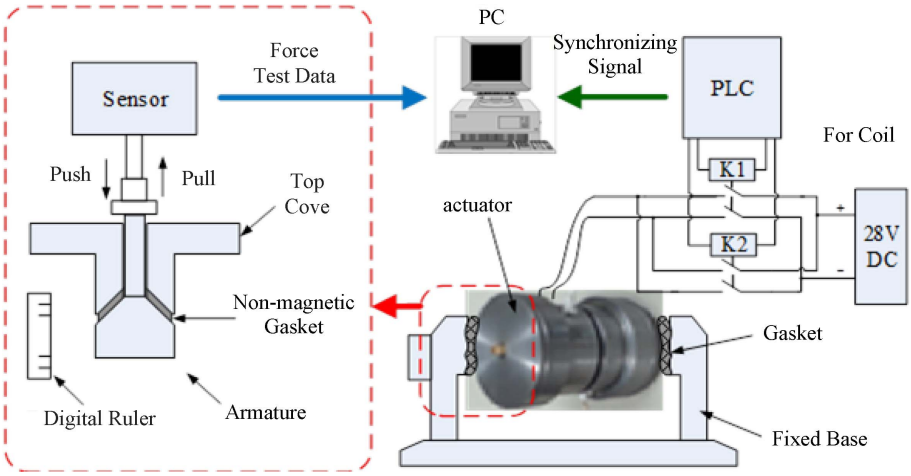

Fig. 13. (Color online) Themeasuring system for the actuator and the prototype actuator.

observed that there is a difference between LPAM and others results when the coils are in an energized state, which occurs when

1) The fan-shaped PM analytical model by LPAM is simply considered as a magnetic resistance and potential, which cannot fully embody the characteristic of the PM in a simplified equivalent magnetic circuit;

2) The fan-shaped PM is considered as the superposition of several magnetic potentials and permeances by MFLD, and the improved equivalent magnetic circuit based on this PM model have contributed to improving the accuracy.

The measuring system for the actuator and the prototype are shown in Fig. 13. MFLD has a good performance on the actuator.

5. Conclusion

This paper has presented an analytical method for magnetic field lines distribution of open-circuit fan-shaped PMs and calculated the leakage permeance using the magnetic field lines distribution. The proposed method involves mapping the magnetic field lines by arc formulae based on the superposition principle of the magnetic field, which presents gradient changes for fan-shaped PMs with different heights. The positions of segmented PMs can then be obtained using the magnetic field lines distribution. Comparing the FEA and LPAM results with the results of the proposed method illustrate the MFLD's accuracy. Furthermore, the proposed method has the advantage of a low computational time. As an example of the practical use of MFLD, an electromagnetic actuator model based on magnetic field line distribution has been built to obtain the latching and output force under different levels of excitation. The MFLD can be validated by comparing the simulated, measured, and calculated results.

Acknowledgment

This work was supported in part by the NSFC (National Natural Science Foundation of China) under Project 51507033. It was also supported in part by China Postdoctor Science Foundation 2016M591530.

References

[1] H. William and J. A. Buck, Engineering Electromagnetics, The MacGraw-Hill Companies, Inc. Arizona (2009) pp. 120-129.
[2] L. X. Bi, S. M. Wang, and Y. H. Xia, J. Tsinghua Univ (Science and Technology). **50**, 4 (2010).
[3] D. Wu, Z. X. Yan, J. L.Yu, and C. Y. Chen, Chinese J. Aero. **26**, 4 (2013).
[4] Z. Mouton and M. J. Kamper, IEEE Tran. Ind. Electron. **61**, 7 (2014).
[5] B. Manz, M. Benecke, and F.Volke, J. Magn. Reson. **192**, 1 (2008).
[6] W. Y. Yang and G. F. Zhai, J. Magn. **19**, 1 (2014).
[7] H. M. Liang, J. B.Lin, and G. F. Zhai, IEICE Trans. Elect. **127**, 11 (2006).
[8] H. M. Liang, J. X. You, Z. W. Cai, and G. F. Zhai, IEICE Trans. Elect. **97**, 12 (2014).
[9] L. Wang, G. X. Li, C. L. Xi, X. J. Wu, and S. P. Sun, Energy Convers. Mgt. **127**, 1 (2016).
[10] Z. Y. Sun, G. X. Li, L. Wang, W. H. Wang, Q. X. Gao, and J. Wang, Energy Convers. Mgt. **113**, 4 (2016).
[11] E. Kurt, H. Gör, and M. Demirtas, Energy Convers. Mgt. **77**, 2 (2014).
[12] F. Daldaban and N. Ustkoyuncu, Energy Convers. Mgt. **49**, 11 (2008).
[13] T. S. Birch and O. I. Butler, Proc. of Ins. of Elec. Eng.

118, 1 (1971).
[14] X. H. Bao, C. Di, and Y. Fang, J. Elec. Eng. Technol. **11**, 1 (2016).
[15] W. L. Li, K. T. Chau, C. H. Liu, S. Gao, and D. Y. Wu, IEEE Trans. Magn. **49**, 7 (2013).
[16] X. Ke, X. D. Yu, M. Shen, D. X. Xie, and B. D. Bai, IEEE Trans. Energy Conversion **52**, 3 (2016).
[17] A. Kohara, K. Hirata, N. Niguchi, and Y. Ohno, IEEE Trans. Magn. **52**, 9 (2016).
[18] B. J. H. de Bruyn, J. W. Jansen, and E. A. Lomonova, IEEE Trans. Magn. **52**, 7 (2016).
[19] F. Meng, H. Zhang, D. P. Cao, and H. Y. Chen, IEEE Trans. Mech. **52**, 7 (2016).
[20] Z.Tanasic, T. Werder, and J. Smajic, IEEE Trans. Magn. **59**, 9 (2016).
[21] Y. Zhou, H. S. Li, G. W. Meng, S. Zhou, and Q. Cao, IEEE Tran. Ind. Electron. **62**, 6 (2015).
[22] N. Gabdullin and S. H. Khan, IEEE Trans. Magn. **59**, 9 (2016).
[23] J. Dusek, P. Arumugam, C. Brunson, E. K. Amankwah, T. Hamiti, and C. Gerada, IEEE Trans. Magn. **52**, 4 (2016).
[24] Y. S. Sun and S. J. Wang, Calculation and Analysis of DC Magnetic System. National Defense Industry Press. Beijing (1987) pp. 26-31.
[25] H. M. Liang, J. X. You, F. B. Luo, W. Y. Yang, and G. F. Zhai, Proc. Chinese. Elect. Eng. **34**, 9 (2014).
[26] J. X. You, Research on Distributed Parameters Model of Nonlinear Permanent Magnet and Its Application in Bridge Magnetic System, Harbin. Inst. Tech. Hei Long Jiang (2014) pp. 19-27.
[27] J. Z. Yi, Magnetic Field Calculation and Magnetic Circuit Design. Chengdu Institute of Telecommunication-Press. Chengdu (1987) pp. 5-20.